Ultrafast Brain Magnetic Resonance Imaging in Acute Neurological Emergencies

Diagnostic Accuracy and Impact on Patient Management

Philipp M. Kazmierczak, MD, Max Dührsen, MS,* Robert Forbrig, MD,† Maximilian Patzig, MD,† Matthias Klein, MD,‡ Andreas Pomschar, MD,§ Wolfgang G. Kunz, MD,* Daniel Puhr-Westerheide, MD,* Jens Ricke, MD,* Olga Solyanik, MD,* and Clemens C. Cyran, MD**

Objectives: The aim of this study was to investigate diagnostic accuracy and impact on patient management of an ultrafast (4:33 minutes/5 sequences) brain magnetic resonance imaging (MRI) protocol for the detection of intracranial pathologies in acute neurological emergencies.

Materials and Methods: Four hundred forty-nine consecutive emergency patients with acute nontraumatic neurological symptoms were evaluated for this institutional review board–approved prospective single-center trial. Sixty patients (30 female, 30 male; mean age, 61 years) with negative head CT were included and underwent emergency brain MRI at 3 T subsequent to CT. MRI included the ultrafast protocol (ultrafast-MRI; sag T1 GRE, ax T2 TSE, ax T2 TSE Flair, ax T2* EPI-GRE, ax DWI SS-EPI; TA, 5 minutes) and an equivalent standard-length protocol (TA, 15 minutes) as reference standard. Two blinded board-certified neuroradiologists independently analyzed the MRI with regard to image quality (1, nondiagnostic; 2, substantial artifacts; 3, satisfactory; 4, minor artifacts; 5, no artifacts) and intracranial pathologies. Sensitivity and specificity for the detection of intracranial pathologies were calculated accordingly.

Results: Ninety-three additional intracranial lesions (acute ischemia, n = 21; intracranial hemorrhage/microbleeds, n = 27; edema, n = 2; white matter lesion, n = 38; chronic infarction, n = 3; others, n = 2) were detected by ultrafast-MRI, whereas 101 additional intracranial lesions were detected by the standard-length protocol (acute ischemia, n = 24; intracranial hemorrhage/microbleeds, n = 32; edema, n = 2; white matter lesion, n = 38; chronic infarction, n = 3; others, n = 2). Image quality was equivalent to the standard-length protocol. Ultrafast-MRI demonstrated high diagnostic accuracy (sensitivity, 0.939 [0.881–0.972]; specificity, 1.000 [0.895–1.000]) for the detection of intracranial pathologies. MRI led to a change in patient management in 10% compared with the initial CT.

Conclusions: Ultrafast-MRI enables time-optimized diagnostic workup in acute neurological emergencies at high sensitivity and specificity compared with a standard-length protocol, with direct impact on patient management. Ultrafast MRI protocols are a powerful tool in the emergency setting and may be implemented on various scanner types based on the optimization of individual acquisition parameters.

Key Words: ultrafast MRI, neurological emergencies, diagnostic accuracy, patient management

(*Invest Radiol* 2020;00: 00–00)

Acute neurological symptoms are among the main reasons for hospital presentation and admission, with a reported percentage of 15% in a general emergency department patient population.[1] Because the most common underlying causes include ischemia, headache disorders, seizures, and intracranial hemorrhage, an accurate and timely diagnosis is crucial for therapy guidance.[2] In the majority of institutions, computed tomography (CT) of the head is the imaging modality of choice to exclude intracranial pathologies in the emergency setting, as it is fast and widely available.[3] State-of-the-art multirow detector CT scanners allow for the acquisition of comprehensive stroke protocols including noncontrast CT, CT angiography, and whole-brain perfusion imaging within minutes.[4] Despite the high diagnostic standard of modern CT, magnetic resonance imaging (MRI) remains the reference standard for the detection and differential diagnosis of intracranial pathologies. However, long acquisition times for multisequence protocols and the potentially resulting delay in diagnosis and treatment limit the use of MRI in the acute setting.

In recent years, several novel MRI technologies significantly accelerating acquisition speed were introduced into clinical routine.[5,6] Modern scanners, optimization of sequence parameters, and the use of parallel imaging techniques now enable the acquisition of an ultrafast brain MRI protocol including 5 standard sequences in only 4:33 minutes, including a 14-second localizer (ultrafast-MRI, including sagittal T1-weighted gradient echo [GRE], axial T2-weighted turbo spin echo [TSE], axial T2-weighted TSE fluid-attenuated inversion recovery [FLAIR], axial diffusion-weighted [DW] single-shot echo-planar imaging [EPI], axial T2*-weighted EPI-GRE). Hence, ultrafast-MRI overcomes the aforementioned limitation of long acquisition times and may be investigated in the acute setting.[7]

The primary objective of this prospective study was to validate ultrafast-MRI for routine use in acute neurological emergencies. Second, we aimed to investigate the impact of ultrafast-MRI on patient management. We therefore hypothesized that

a. image quality and diagnostic performance of ultrafast-MRI for the detection of intracranial pathologies are noninferior to the standard-length brain MRI protocol
b. ultrafast-MRI leads to a change in patient management compared with CT alone.

Received for publication July 26, 2019; and accepted for publication, after revision, September 4, 2019.

From the *Department of Radiology, †Institute of Neuroradiology, and ‡Department of Neurology, University Hospital, LMU Munich; and §DIE RADIOLOGIE, München, Germany.

Conflicts of interest and sources of funding: This study was supported by a research grant from Siemens Healthineers.

Olga Solyanik and Clemens C. Cyran contributed equally and share last authorship.

Correspondence to: Philipp M. Kazmierczak, MD, Department of Radiology, University Hospital, LMU Munich, Marchioninistraße 15, 81377 München, Germany. E-mail: philipp.kazmierczak@med.lmu.de.

ISSN: 0020-9996/20/0000–0000
DOI: 10.1097/RLI.0000000000000625

MATERIALS AND METHODS

Study Design and Patients

This prospective single-center diagnostic accuracy study was performed with institutional review board approval, and all included patients provided written informed consent to participate in the study. Between January and October 2018, 449 consecutive patients with acute nontraumatic neurological symptoms presented to our emergency department during the MRI slots reserved by our workgroup. Two hundred thirty-eight patients underwent head CT due to suspected intracranial pathology. If the CT scan showed no sufficient explanation for the acute symptoms, patients were included and subsequently transferred to the

TABLE 1. Inclusion and Exclusion Criteria

Inclusion Criteria	Exclusion Criteria
≥18 y	<18 y
Acute neurological symptoms	CT correlate of the symptoms
Suspected intracranial pathology	Intravenous thrombolysis/mechanical recanalization
No explanation for the symptoms by CT	Unstable clinical condition
Informed consent	Inability to consent
	Pregnancy

3 T MRI suite (MAGNETOM Skyra; Siemens Healthineers, Erlangen, Germany). The mean time interval between the head CT examination and the MRI scan was 153.4 ± 98.7 minutes. Detailed inclusion and exclusion criteria are provided in Table 1. A total of 60 patients (30 female, 30 male; mean age, 61 years) were successfully included. The flowchart of patient inclusion is shown in Figure 1. Clinical characteristics of the included patients are listed in Table 2.

MRI Protocol

All examinations were performed using a 20-channel receiver head coil. Two brain MRI protocols, each including the below-mentioned 5 standard sequences, were acquired in randomized order. Ultrafast-MRI is a vendor-specific, commercially available protocol (GOBrain; Siemens Healthineers, Erlangen, Germany), which was additionally optimized for the use on our MRI scanner. The standard-length protocol served as reference standard. Individual acquisition times are displayed in parentheses for both ultrafast-MRI and the standard-length protocol:

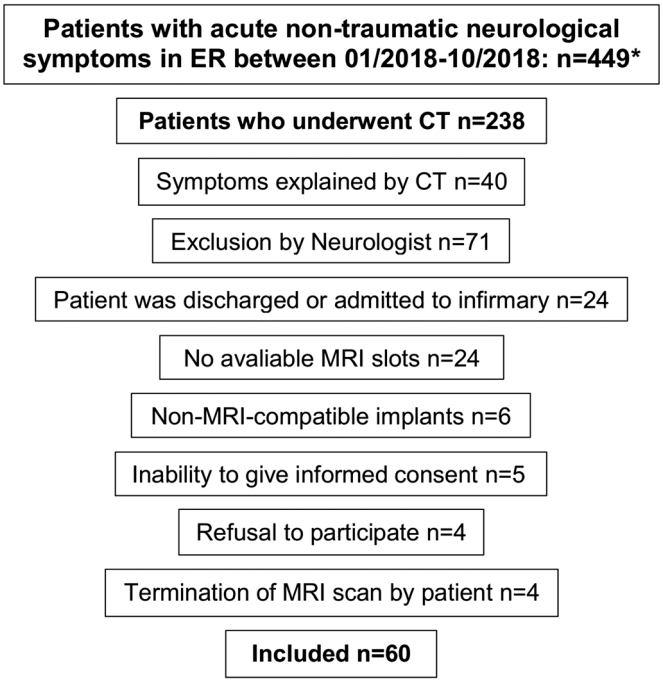

FIGURE 1. Patient inclusion flowchart. The majority of patients (111/238) were excluded due to sufficient explanation of symptoms by CT (n = 40) or due to clinical reasons (ie, exclusion by neurologist, n = 71; for example, initiated intravenous thrombolysis or cardiorespiratory instability).

TABLE 2. Neurological Symptoms

Characteristic	Value
Age, mean ± SD (range), y	61 ± 19 (22–91)
Male/female	30/29
Body mass index (mean ± SD)	26.0 ± 4.4
Vertigo	23
Paresthesia	16
Cephalgia	14
Impaired vision	14
Aphasia	13
Motor deficit	9
Memory impairment	3
Urinary dysfunction	2
Tremor	2
Double vision	1

1. Sagittal T1-weighted GRE (ultrafast-MRI 41 seconds; standard-length: 1:34 minutes)
2. Axial T2-weighted TSE (ultrafast-MRI 1:02 minutes; standard-length: 3:45 minutes)
3. Axial T2-weighted TSE FLAIR (ultrafast-MRI 1:52 minutes; standard-length: 4:02 minutes)
4. Axial T2*-weighted EPI-GRE (ultrafast-MRI 6 seconds; standard-length: 4:44 minutes)
5. Axial DWI SS-EPI (ultrafast-MRI 38 seconds; standard-length: 1:06 minutes)

Total acquisition times were 4:19 minutes for ultrafast-MRI and 15:11 minutes for the standard-length protocol, respectively. The same localizer (14 seconds) was used for both protocols, and the total acquisition time for the 2 protocols was 19 minutes 44 seconds. Individual sequence parameters of the 2 protocols are provided in Tables 3 and 4. Briefly, ultrafast-MRI is based on the optimization of individual sequence parameters and the use of parallel imaging with higher acceleration factors (generalized autocalibrating partially parallel acquisition [GRAPPA]), gradient echo T1-weighted and EPI-GRE T2*-weighted sequences, and the elimination of manual intersequence adjustments.

Image Reading

All Digital Imaging and Communications in Medicine (DICOM) data sets were anonymized before randomization. Two blinded board-certified neuroradiologists (each with 8 years of experience in diagnostic neuroradiology) independently analyzed the image data sets on a dedicated workstation using an open-source medical image viewer (Horos v2.1.1; The Horos Project). The reading was performed blinded, in randomized order, and in several reading sessions. The ultrafast and the standard-length protocol were read separately, and the sequences were analyzed side-by-side with the other sequences of the respective MRI protocol. Image quality of the standard and the ultrafast MR protocol was assessed on a 5-point Likert scale: 1, nondiagnostic; 2, substantial artifacts; 3, satisfactory; 4, minor artifacts; 5, no artifacts.[7] Analogous to Prakkamakul et al,[7] the gray-white matter differentiation as marker of image quality was evaluated on T1-weighted, T2-weighted, and FLAIR images using a 3-point scale (0, no visible gray-white matter differentiation; 1, unclear but recognizable borders; 2, clear differentiation). In case of divergent results, a consensus reading was performed by a third reader.

Assessment of Diagnostic Accuracy

To calculate the parameters of diagnostic accuracy for ultrafast-MRI, the image data sets were read regarding 6 intracranial pathology

TABLE 3. Sequence Parameters of Ultrafast-MRI

Ultrafast-MRI					
			Total Exam Time, min: 4:19		
Sequence Parameter	**T1 GRE**	**T2 TSE**	**T2 TSE DarkFluid (FLAIR)**	**ep2d Diffusion**	**ep2d T2*w**
Plane	Sagittal	Axial	Axial	Axial	Axial
TR, ms	240	6200	8000	4200	6120
TE, ms	2.46	78	119	74	30
Flip angle, degrees	80	120	150	90	90
TI, ms	—	—	2370	—	—
FOV, mm	220	220	220	240	220
FOV phase, %	100	87.5	87.5	100	100
Base resolution, mm	256	256	256	160	256
Phase resolution, %	81	98	98	100	100
ST, mm	4.0	5.0	5.0	5.0	5.0
Voxel size, mm^3	0.9 × 0.9 × 4.0	0.9 × 0.9 × 5.0	0.9 × 0.9 × 5.0	1.5 × 1.5 × 5.0	0.9 × 0.9 × 5.0
Slice number	35	25	25	25	25
TA, min	00:41	01:02	01:52	00:38	00:06
Respiratory control	Off	Off	Off	Off	Off
Bandwidth, hertz per pixel	360	260	287	1200	1500
Phase oversampling, %	40	0	25	0	0
Parallel Imaging	GRAPPA	GRAPPA	GRAPPA	GRAPPA	None
Acceleration Factor	2	3	2	2	None
Multislice mode	Interleaved	Interleaved	Interleaved	Interleaved	Interleaved

GRE indicates gradient echo; TSE, turbo spin echo; FLAIR, fluid-attenuated inversion recovery; TR, repetition time; TE, echo time; FOV, field of view; FS, fat saturation; ST, slice thickness; TA, acquisition time; GRAPPA, generalized autocalibrating partially parallel acquisition.

TABLE 4. Sequence Parameters of the Standard-Length Protocol

Standard-Length Protocol					
			Total Exam Time, min: 15:11		
Sequence Parameter	**T1 GRE**	**T2 TSE**	**T2 TSE DarkFluid (FLAIR)**	**ep2d Diffusion**	**ep2d T2*w**
Plane	Sagittal	Axial	Axial	Axial	Axial
TR, ms	240	6200	8000	5900	501
TE, ms	2.46	78	122	98	19.9
Flip angle, degrees	80	150	180	90	20
TI, ms	—	—	2366.9	—	—
FOV, mm	220	220	220	220	220
FOV phase, %	100	100	100	100	100
Base resolution, mm	320	384	320	192	320
Phase resolution, %	81	100	70	100	80
ST, mm	4.0	5.0	5.0	5.0	5.0
Voxel size, mm^3	0.7 × 0.7 × 4.0	0.6 × 0.6 × 5.0	0.7 × 0.7 × 5.0	0.6 × 0.6 × 5.0	0.7 × 0.7 × 5.0
Slice number	35	25	25	25	25
TA, min	01:34	03:45	04:02	01:06	04:44
Respiratory control	Off	Off	Off	Off	Off
Bandwidth, hertz per pixel	360	260	180	1042	200
Phase oversampling, %	40	10	0	0	10
Parallel Imaging	GRAPPA	None	None	GRAPPA	None
Acceleration Factor	2	—	—	2	—
Multislice mode	Interleaved	Interleaved	Interleaved	Interleaved	Interleaved

GRE indicates gradient echo; TSE, turbo spin echo; FLAIR, fluid-attenuated inversion recovery; TR, repetition time; TE, echo time; FOV, field of view; FS, fat saturation; ST, slice thickness; TA, acquisition time; GRAPPA, generalized autocalibrating partially parallel acquisition.

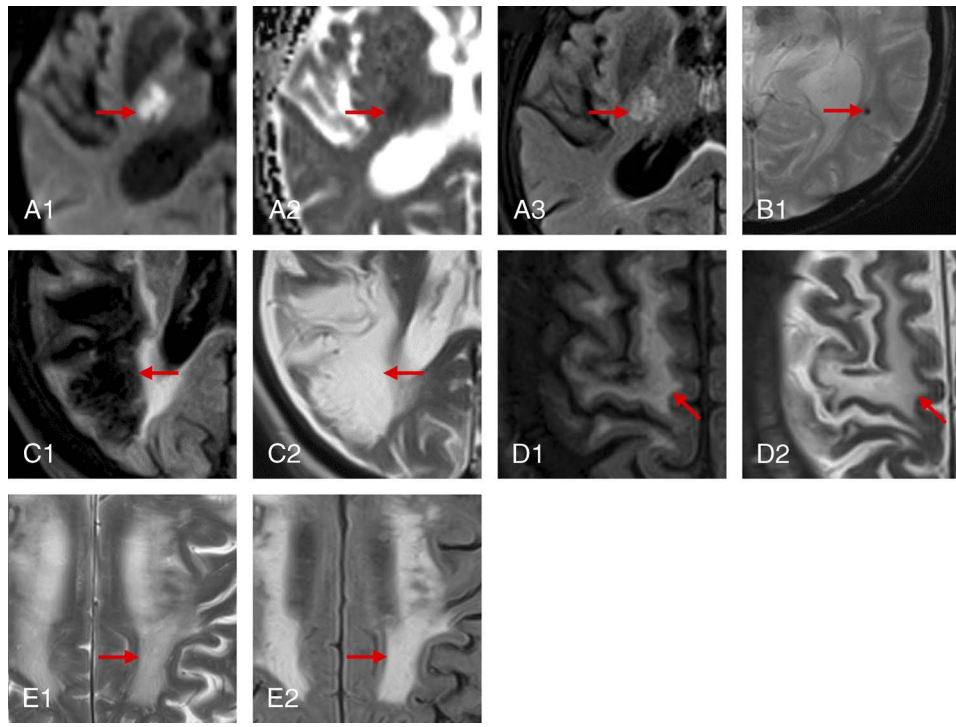

FIGURE 2. Intracranial pathology categories. Representative images. Pathologies indicated by arrows. A, Acute ischemia, hyperintense in diffusion-weighted imaging (DWI, A1), hypointense in ADC (A2), hyperintense in fluid-attenuated inversion recovery (FLAIR, A3). B, Microbleed, T2*-hypointense. C, Chronic infarction: cystic transformation hypointense in fluid-attenuated inversion recovery (FLAIR, C1) and hyperintense in T2 (C2). Note the isointense gliotic rim (C1), D, Edema, hyperintense in both fluid-attenuated inversion recovery (FLAIR, D1) and T2 (D2). E, White matter lesions: confluent T2 (E1) and fluid-attenuated inversion recovery (FLAIR, E2) hyperintense lesions.

categories: acute ischemia, chronic infarction, intracranial hemorrhage/microbleeds, edema, white matter lesion, and miscellaneous. The 6 intracranial pathology categories were defined as follows (image examples provided in Fig. 2):

1. Acute ischemia: diffusion restriction (DWI-hyperintense), apparent diffusion coefficient (ADC)–hypointense with or without FLAIR hyperintensity
2. Chronic infarction: no diffusion restriction, hyperintensity (gliosis/cystic transformation) in FLAIR/T2
3. Intracranial hemorrhage/microbleeds: T2*-hypointense, intracranial hematomas with T1 and T2 signal according to their respective age
4. Edema: hyperintense in FLAIR/T2, with or without focal or generalized swelling of brain parenchyma
5. White matter lesion: FLAIR/T2-hyperintense lesions in the white matter, may be confluent
6. Miscellaneous: any other lesion not matching the aforementioned definitions (1–5)

For both ultrafast-MRI and the standard-length protocol, a consensus reading was performed in case of divergent reading results.

Statistical Analysis

Statistical analysis was performed using a commercially available statistics software (SAS Version 9.4 for Windows, SAS Institute Inc, Cary, NC). Sensitivity and specificity of ultrafast-MRI were calculated against the standard-length protocol that served as reference standard. Interrater agreement was calculated using Cohen's k. Cohen's k values were interpreted as follows: 0.00–0.20, slight agreement; 0.21–0.40, fair agreement; 0.41–0.60, moderate agreement; 0.61–0.80, substantial agreement; and >0.80, high agreement.[8] Assessments of image quality and gray-white matter differentiation were compared using McNemar test.

RESULTS

Due to severe motion artifacts, one patient was excluded. In total, 59 patients were successfully included for statistical analysis.

Qualitative Analysis

Image quality of ultrafast-MRI was equivalent to the standard-length protocol. Results of image quality and GM-WM differentiation assessments are listed in Table 5. Interobserver agreement for the image quality was high for T1-weighted sequences and diffusion imaging and slight or fair for other sequences. Interobserver agreement for gray-white matter differentiation was substantial for all sequences (Table 6).

Diagnostic Accuracy

Compared with CT, 93 additional intracranial lesions were detected by ultrafast-MRI (acute ischemia, n = 21; intracranial hemorrhage/microbleeds, n = 27; edema, n = 2; white matter lesion, n = 38; chronic infarction, n = 3; others, n = 2) while 101 additional intracranial lesions were detected by the standard-length protocol (acute ischemia, n = 24; intracranial hemorrhage/microbleeds, n = 32; edema, n = 2; white matter lesion, n = 38; chronic infarction, n = 3; others, n = 2). Ultrafast-MRI demonstrated high diagnostic accuracy with a sensitivity of 0.939 (95% confidence interval, 0.881–0.972) and a specificity of 1.000 (95% confidence interval, 0.895–1.000) for the detection of intracranial pathologies. Figures 3, 4, and 5 show exemplary cases in which ultrafast-MRI proved to be equivalent to the standard-length protocol. Figure 6 summarizes the cases in which more lesions were detected based on the standard-length protocol. Magnetic resonance imaging led to a change

TABLE 5. Results of Image Quality and GM-WM Differentiation Assessments (Consensus Reading)

	Image Quality						GM-WM Differentiation			
	Scores						Scores			
Sequences	1	2	3	4	5	Median	0	1	2	Median
T1-weighted										
Conventional	0	0	1	58	0	4	0	6	53	2
Ultrafast	0	0	0	59	0	4	0	7	52	2
T2-weighted										
Conventional	0	0	3	54	2	4	0	34	25	1
Ultrafast	0	0	2	57	0	4	0	39	20	1
FLAIR										
Conventional	0	0	2	56	1	4	0	32	27	1
Ultrafast	0	0	1	58	0	4	0	31	28	1
DWI										
Conventional	0	0	0	59	0	4	NA	NA	NA	NA
Ultrafast	0	0	0	59	0	4	NA	NA	NA	NA
T2*										
Conventional	0	0	6	53	0	4	NA	NA	NA	NA
Ultrafast	0	2	56	1	0	3	NA	NA	NA	NA

NA indicates not applicable; GM-WM, gray-white matter.

in patient management in 10% (6/59): admission to a dedicated stroke unit in 6 of 59 patients and initiation of acetyl-salicylic acid treatment for secondary stroke prophylaxis in 3 of 6 stroke unit patients.

Lesions Not Detected by Ultrafast-MRI

Eight lesions (ischemia, n = 3; hemorrhage/microbleeds, n = 5) were only detected based on the standard-length protocol (the discrepant imaging findings are shown in Figure 6). However, the 3 diffusion restrictions were visible on both protocols but due to low signal intensity on ultrafast-MRI only judged as acute ischemia in the standard-length protocol. Three subtle microbleeds were visible on both protocols but only read in the standard-length protocol due to low susceptibility on ultrafast-MRI. Due to lower resolution, 2 adjacent microbleeds were read as one on ultrafast-MRI. One microbleed was not visible on ultrafast-MRI due to low resolution as well as preexisting hemosiderin deposits in the basal ganglia.

DISCUSSION

In this prospective study, we investigated an ultrafast, 4:33 minutes/5 sequences brain MRI protocol for the detection of intracranial pathologies in acute neurological emergencies. It was demonstrated that image quality and diagnostic performance of ultrafast-MRI are noninferior to the standard-length brain MRI protocol. In addition, MRI led to a change in patient management in 10%. Our data provide evidence for the standard use of ultrafast-MRI as alternative to CT for the detection and differential diagnosis of intracranial pathologies in acute neurological emergencies.

The results of our prospective study are in line with a recent retrospective study by Prakkamakul et al[7] who investigated this vendor-specific ultrafast brain MRI protocol in neurological/neurosurgical intensive care unit patients who had a high likelihood for motion artifacts due to altered mental status or restlessness. The authors compared image quality, gray-white matter differentiation, and concordance for 6 clinically relevant imaging findings between ultrafast-MRI and a conventional protocol (acquisition time 10:32 minutes). Ultrafast-MRI and the conventional protocol showed comparable image quality and high concordance (85%) for the key imaging findings. Another group prospectively investigated an ultrafast brain MRI protocol in a pediatric patient population with potential abusive head trauma.[9] They found the ultrafast protocol to yield low sensitivity for intracranial traumatic changes compared with the standard-length protocol serving as reference standard. However, in contrast to the standard-length protocol, the ultrafast scan was performed without sedation or general anesthesia, which limits the comparability of the 2 protocols in a pediatric patient population due to motion artifacts. Apart from these 2 studies, several additional investigations of ultrafast brain MRI protocols have been published.[10–12] The acquisition time of the investigated sequences and protocols ranged from 1 to 10 minutes, and rapid acquisition was either enabled by modern MRI technologies with optimized scan parameters or synthetic MRI. The studies focused on feasibility of ultrafast MRI protocols in clinical routine without prospectively investigating the diagnostic accuracy of ultrafast MRI in an emergency setting. However, prospective diagnostic accuracy studies are necessary to confirm ultrafast-MRI as valid alternative to CT in the emergency setting and in order to exclude a loss of relevant information compared with the reference standard when using an ultrafast protocol. Our data add to the field as we demonstrated the noninferiority of ultrafast-MRI to a standard-length protocol with regard to image quality and diagnostic performance, as well as the impact on clinical decision making compared with our institutional emergency imaging standard, CT. Thus, ultrafast-MRI can be used as the imaging modality of choice for the emergency diagnostic-workup of selected neurological patients with

TABLE 6. Interrater Agreement

Parameters	Interobserver Agreement		95% CI	
	Ultrafast	Conventional	Ultrafast	Conventional
Image quality				
T1-weighted	1.0	1.0	1.0	1.0
T2-weighted	0.37	−0.02	−0.18 to 0.93	−0.06 to 0.02
FLAIR	−0.01	−0.02	−0.02 to 0.004	0.06 to −0.26
DWI	1.0	1.0	1.0	1.0
T2*-weighted	0.11	0.32	−0.10 to 0.3	0.001 to 0.65
GM-WM differentiation				
T1-weighted	0.71	0.83	0.45 to 0.98	0.61 to 1.00
T2-weighted	0.60	0.49	0.37 to 0.83	0.24 to 0.72
FLAIR	0.66	0.69	0.46 to 0.85	0.50 to 0.87

GM-WM indicates gray-white matter.

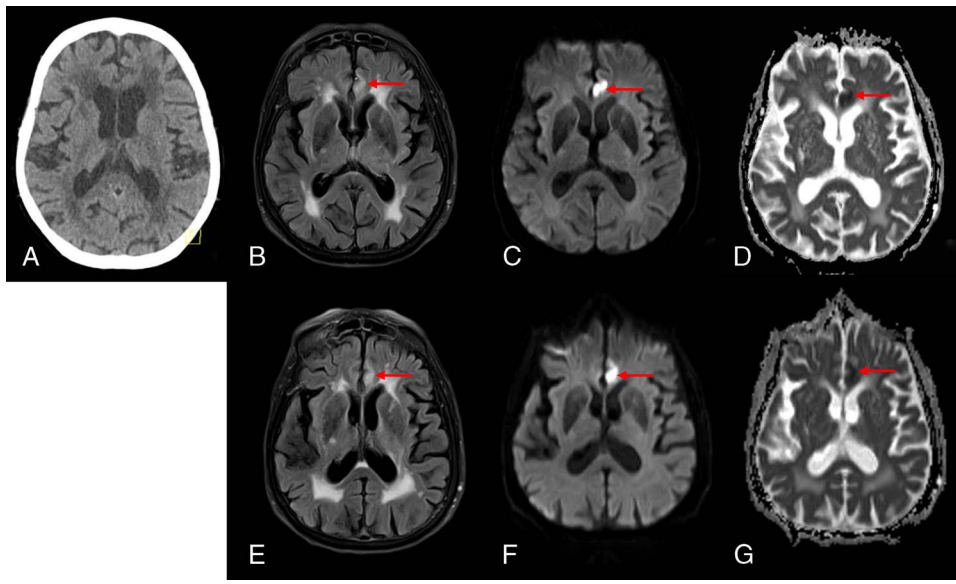

FIGURE 3. CT-occult subacute ischemia (left gyrus cinguli). Axial noncontrast head CT (A), fluid-attenuated inversion recovery (FLAIR) (B and E), diffusion-weighted imaging (DWI) (C and F), ADC-map (D and G) from the standard-length protocol (top row) and ultrafast-MRI (bottom row) in an 83-year-old woman with known epilepsy presenting with somnolence. The noncontrast head CT showed no evidence of ischemia or hemorrhage. Magnetic resonance imaging demonstrated a small subacute ischemic lesion in the left gyrus cinguli (arrow). Ultrafast-MRI demonstrated noninferior image quality and lesion conspicuity compared with the standard-length protocol.

suspected intracranial pathologies. Depending on the suspected pathology and based on the initial imaging results in the acute setting, the ultrafast-MRI protocol may be individualized by appending further sequences. Possible protocol extensions include dedicated brain stem DWI or constructive interference in steady state sequences for optimized diagnosis of infratentorial pathologies, contrast-enhanced T1-weighted for suspected tumor or neuroinflammatory disease, or MR angiography (eg, time-of-flight [TOF] or contrast-enhanced) to exclude vascular pathologies. As cerebrovascular disease is among the main causes of neurological emergency department admission, particularly MR angiography is a valuable completion of ultrafast brain MRI protocols. Depending on the technique, MR angiography scans may be performed within minutes and allow for the detection of vessel occlusions, aneurysms, direct signs of arterial dissections, or sinus/cerebral vein thrombosis.

The lesions not detected by ultrafast-MRI did not have any clinical consequence, as all of these patients demonstrated at least one other ischemic lesion or microbleed. We must acknowledge that TA (ultrafast-MRI) was only 6 seconds for T2* and 38 seconds for DWI, respectively.

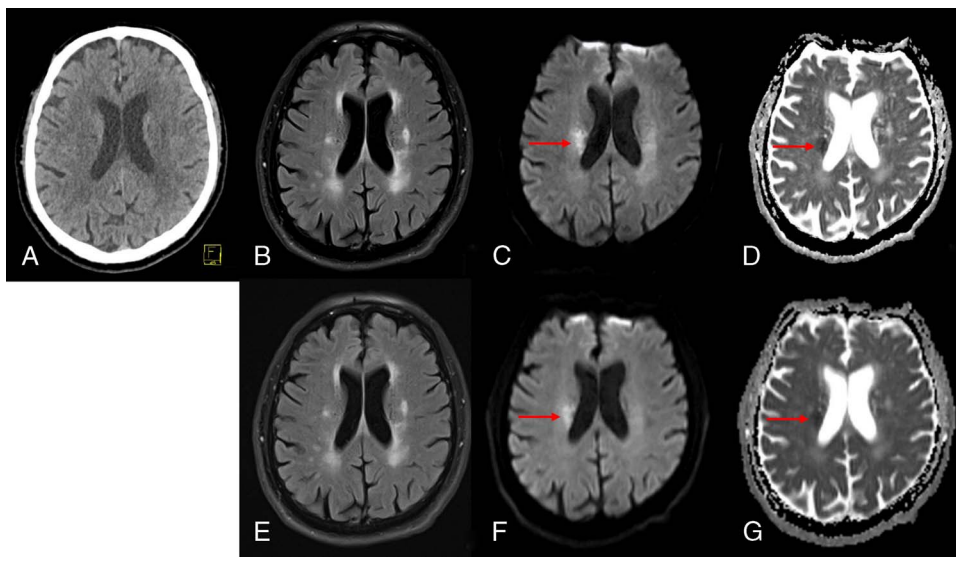

FIGURE 4. CT-occult acute ischemia (right corona radiata). Axial noncontrast head CT (A), fluid-attenuated inversion recovery (FLAIR) (B and E), diffusion-weighted imaging (DWI) (C, F), ADC-map (D and G) from the standard-length protocol (top row) and ultrafast-MRI (bottom row) in a 72-year-old man presenting with acute left facial paralysis, dysarthria, and left-body coordination disorder. The noncontrast head CT showed no evidence of ischemia or hemorrhage. Magnetic resonance images showed acute focal infarction in the right internal capsule and the corona radiata (arrow). The images show the comparable quality and lesion conspicuity in the ultrafast protocol, compared with the conventional protocol.

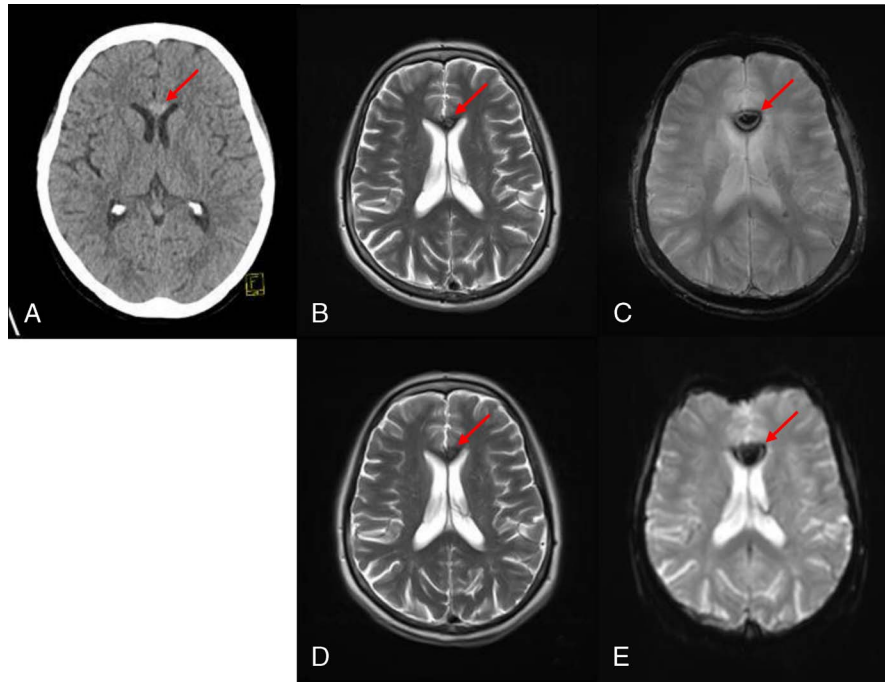

FIGURE 5. Incidental cavernoma (genu of the corpus callosum). Axial noncontrast head CT (A), axial T2 TSE (B and D), axial T2* (C and E) from the standard-length protocol (top row) and ultrafast-MRI (bottom row) of a 62-year-old woman reporting visual disturbance of the right eye for about 15 to 30 minutes. Neither CT nor MRI showed a correlate for the symptoms. However, noncontrast CT demonstrated a hyperdense lesion in the genu of the corpus callosum (A, arrow) not in line with acute hemorrhage. Based on the subsequently acquired MRI, this lesion could be diagnosed as incidental cavernoma, demonstrating the typical low to intermediate T2 signal (B and D, arrow) and susceptibility artifacts (B–E, arrow). No developmental venous anomaly. This is a classic case in which the patient would have been referred to an outpatient MRI unit for further diagnostic workup of the hyperdense lesion a few days later. However, ultrafast-MRI was able to deliver the final diagnosis during initial presentation to the emergency department in a one-stop-shop manner.

For clinical application, TA of the 2 sequences may be increased in order to gain signal intensity (DWI), susceptibility (T2*), and resolution (T2*) without significantly adding to the total acquisition time of ultrafast-MRI. For instance, the TA of the conventional DWI sequence was 1:06 minutes and therefore only 28 seconds longer compared with the DWI sequence of ultrafast-MRI. Hence, the conventional DWI may be used in the ultrafast protocol without significantly adding to the TA. Taking into consideration the importance of ischemia detection in the emergency setting, this may represent a valuable protocol adjustment.

It must be noted that MRI may not be the optimal imaging modality for every acute neurological emergency patient. Due to high water content and therefore prolonged T1 times, hyperacute intracranial hematomas may be isointense to brain tissue on T1-weighted images and indistinguishable from other water-containing structures (eg, tumors with surrounding edema) on T2-weighted images.[13] This may be a limitation especially in subtle bleedings, such as subarachnoid hemorrhage limited to a single sulcus or small contusions. Relative and absolute contraindications to MRI, that is, claustrophobia and non–MRI-conditional intracorporal devices, may further limit the applicability of ultrafast-MRI in individual patients. As a consequence, we suggest that the choice of the optimal imaging modality in the acute situation is made on an individual patient basis. Patients with a high clinical likelihood for intracranial hemorrhage, suspicion of ischemic stroke with eligibility for intravenous thrombolysis, or MRI contraindications should still undergo CT as initial imaging workup.

Magnetic resonance imaging demonstrated a change in patient management when compared with the initial CT. However, it can be assumed that the number of cases in which MRI lead to a change in patient management when compared with CT would be even higher without the preselection in this study setting. The comprehensive stroke protocol includes a CT angiography of the extracranial and intracranial vessels and a whole-brain CT perfusion. As a result, the number of patients without sufficient CT correlate of their neurological symptoms is low. Furthermore, even MRI scans without detection of a pathology provide a high clinical value in the emergency setting. Negative MRI scans facilitate patient management, as they enable the exclusion of relevant intracranial pathologies in a one-stop-shop manner. Given the change in patient management, the time savings compared with the standard protocol, and the acquisition of one fast MRI scan instead of a CT in the acute situation and a standard-length MRI scan a few days later, ultrafast-MRI may be more cost-effective than emergency CT in this patient population. Hence, cost-effectiveness of ultrafast-MRI should be investigated in future studies.

Limitations

We acknowledge several limitations of the study. First, a reading bias cannot be fully excluded as the blinded readers always analyzed both the ultrafast-MRI and the standard-length protocol data sets. Pathologies detected on the standard-length protocol data sets may have influenced the reader to also describe these on ultrafast-MRI, even if subtle. However, we tried to control that potential bias as the reading was performed in randomized order. Second, as outlined previously, there is a preselection bias since the comprehensive CT protocol already detected a substantial number of pathologies. As a result, the patients included in the study presented with subtle changes not visible on CT. In addition, severely ill patients, in which the study MRI would have delayed therapy or the patient transfer to the MRI suite would have posed a risk were excluded. Third, the study was conducted during the weekends and evening hours. As no dedicated emergency department MRI scanner is available at our institution, we had to share the clinical

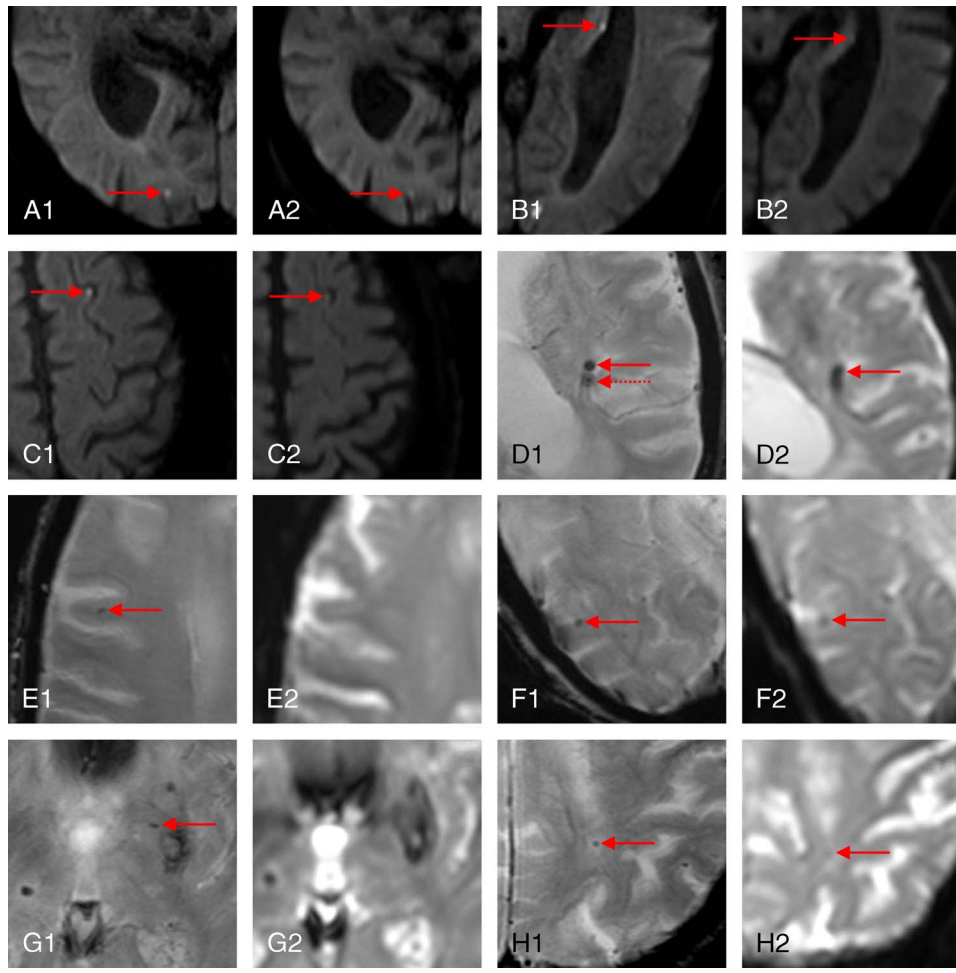

FIGURE 6. Additional lesions in the standard-length protocol compared with ultrafast-MRI. Eight additional lesions (ischemia, n = 3; hemorrhage/microbleeds, n = 5) were detected in the standard-length protocol. A1, B1, C1, DWI/standard-length protocol. A2, B2, C2, DWI/ultrafast-MRI: small focal diffusion restrictions (A, right occipital lobe; B, left hippocampus; C, left superior frontal gyrus) were visible on both the standard-length and ultrafast-MRI. However, due to low signal intensity on ultrafast-MRI, they were only judged as acute ischemia based on the standard-length sequence. D1, E1, F1, G1, H1, T2*/standard-length protocol. D2, E2, F2, G2, H2, T2*/ultrafast-MRI: 3 microbleeds (E, right frontal lobe; F, right occipital lobe; H, left parietal lobe) demonstrated low susceptibility on ultrafast-MRI and were therefore only read in the standard-length protocol. Due to lower resolution, 2 adjacent microbleeds (D, left insula) were read as one on ultrafast-MRI. One microbleed (G, left putamen) was not visible on ultrafast-MRI due to low resolution as well as preexisting hemosiderin deposits in the left basal ganglia.

MRI scanner with other research groups. As an effect, in some patients, there was additional delay between the 2 scans due to temporary unavailability of the MRI scanner, explaining the time interval between the 2 scans. In addition to the aforementioned points, it must be noted that ultrafast MRI protocols are not limited to a single scanner type or vendor. They may be implemented on various scanners and are based on the optimization of individual acquisition parameters.

CONCLUSIONS

Image quality and diagnostic performance for the detection of intracranial pathologies of ultrafast-MRI are equivalent to a standard-length protocol. Ultrafast-MRI thus is a valid alternative to head CT in selected neurological emergency patients and impacts patient management compared with CT alone.

ACKNOWLEDGMENT

The authors thank Dipl.-Stat. Regina Schinner for her kind support regarding the statistical analysis.

REFERENCES

1. Moulin T, Sablot D, Vidry E, et al. Impact of emergency room neurologists on patient management and outcome. *Eur Neurol*. 2003;50:207–214.
2. Rizos T, Juttler E, Sykora M, et al. Common disorders in the neurological emergency room—experience at a tertiary care hospital. *Eur J Neurol*. 2011;18:430–435.
3. Wang X, You JJ. Head CT for nontrauma patients in the emergency department: clinical predictors of abnormal findings. *Radiology*. 2013;266:783–790.
4. Vilela P, Rowley HA. Brain ischemia: CT and MRI techniques in acute ischemic stroke. *Eur J Radiol*. 2017;96:162–172.
5. Runge VM, Richter JK, Heverhagen JT. Speed in clinical magnetic resonance. *Invest Radiol*. 2017;52:1–17.
6. Hagiwara A, Hori M, Cohen-Adad J, et al. Linearity, bias, intrascanner repeatability, and interscanner reproducibility of quantitative multidynamic multiecho sequence for rapid simultaneous relaxometry at 3 T: a validation study with a standardized phantom and healthy controls. *Invest Radiol*. 2019;54:39–47.
7. Prakkamakul S, Witzel T, Huang S, et al. Ultrafast brain MRI: clinical deployment and comparison to conventional brain MRI at 3T. *J Neuroimaging*. 2016;26:503–510.

8. Tang W, Hu J, Zhang H, et al. Kappa coefficient: a popular measure of rater agreement. *Shanghai Arch Psychiatry.* 2015;27:62–67.
9. Kralik SF, Yasrebi M, Supakul N, et al. Diagnostic performance of ultrafast brain MRI for evaluation of abusive head trauma. *AJNR Am J Neuroradiol*. 2017;38: 807–813.
10. Tekes A, Senglaub SS, Ahn ES, et al. Ultrafast brain MRI can be used for indications beyond shunted hydrocephalus in pediatric patients. *AJNR Am J Neuroradiol*. 2018; 39:1515–1518.
11. U-King-Im JM, Trivedi RA, Graves MJ, et al. Utility of an ultrafast magnetic resonance imaging protocol in recent and semi-recent strokes. *J Neurol Neurosurg Psychiatry.* 2005;76:1002–1005.
12. Ryu KH, Choi DS, Baek HJ, et al. Clinical feasibility of 1-min ultrafast brain MRI compared with routine brain MRI using synthetic MRI: a single center pilot study. *J Neurol.* 2019;266:431–439.
13. Parizel PM, Makkat S, Van Miert E, et al. Intracranial hemorrhage: principles of CT and MRI interpretation. *Eur Radiol.* 2001;11:1770–1783.